Plant Mol Biol
DOI 10.1007/s11103-010-9658-8

Intracellular pH sensing is altered by plasma membrane PIP aquaporin co-expression

Jorge Bellati · Karina Alleva · Gabriela Soto · Victoria Vitali · Cintia Jozefkowicz · Gabriela Amodeo

Received: 21 July 2009 / Accepted: 17 June 2010

Abstract The plant plasma membrane barrier can express aquaporins (PIP1 and PIP2) that show two intriguing aspects: (1) the potential of modulating *whole membrane water permeability* by co-expression of both types, which have recently been distinguished for showing a different capacity to reach the plasma membrane; and (2) the faculty to reduce *water permeation through the pore* after cytosolic acidification, as a consequence of a gating process. Our working hypothesis is that these two key features might enhance plasticity of the membrane water transport capacity if they jointly trigger any cooperative interaction. In previous work, we proved by biophysical approaches that the plasma membrane of the halophyte *Beta vulgaris* storage root presents highly permeable aquaporins that can be shut down by acidic pH. Root *Beta vulgaris* PIPs were therefore subcloned and expressed in Xenopus oocytes. Co-expression of *Bv*PIP1;1 and *Bv*PIP2;2 not only enhances oocyte plasma membrane water permeability synergistically but also reinforces pH inhibitory response from partial to complete shut down after cytosolic pH acidification. This pH dependent behavior shows that PIP1–PIP2 co-expression accounts for a different pH sensitivity in comparison with PIP2 expression. These results prove for the first time that PIP co-expression modulates the membrane water permeability through a pH regulatory response, enhancing in this way membrane versatility to adjust its water transfer capacity.

Keywords pH sensing · Plasma membrane intrinsic proteins · Cytosolic acidification · Aquaporin gating

Abbreviations

AQP	Aquaporin
P_f	Osmotic water permeability
PIP	Plasma membrane intrinsic protein (aquaporin)
PM	Plasma membrane
ARCA	Anti-reverse cap analog

Introduction

The plant plasma membrane contains highly specialized proteins for water transport known as PIP aquaporins. PIPs represent one of the largest groups of aquaporins (13 PIP isoforms in both *Zea mays* and *Arabidopsis thaliana*) and all its members share very high identity being concentrated in only two main clusters: PIP1 and PIP2 (Chaumont et al. 2001). This feature is not present in the other plant aquaporin groups (TIP, NIP or SIP) or the more divergent animal ones (AQPs) (Zardoya and Villalba 2001).

PIP isoforms from both clusters have been localized in key organs such as leaves (Hachez et al. 2008), roots (Boursiac et al. 2008; Javot et al. 2003) or fruits (Hu et al. 2003; Picaud et al. 2003; Mut et al. 2008), showing various

J. Bellati · K. Alleva · V. Vitali · C. Jozefkowicz · G. Amodeo
Laboratorio de Biomembranas, Departamento de Fisiología, Facultad de Medicina, Universidad de Buenos Aires, Buenos Aires, Argentina

G. Soto
Instituto de Ingeniería Genética y Biología Molecular (INGEBI-CONICET), Buenos Aires, Argentina

G. Amodeo (✉)
Departamento de Biodiversidad y Biología Experimental, Facultad de Ciencias Exactas y Naturales, UBA, Pabellón II Piso 4 Ciudad Universitaria, C1428EHA Buenos Aires, Argentina
e-mail: amodeo@dna.uba.ar

Published online: 01 July 2010

expression patterns under different developmental and/or environmental situations. Most of the works in the literature emphasizes their crucial role in modulating water transmembrane transfers (Hachez et al. 2006; Maurel et al. 2008).

In order to characterize aquaporins, different biophysical approaches must be employed due to the absence of a direct electrophysiological technique like the ones described for ion channels. One of the key parameters of aquaporin water transport capacity is the membrane osmotic water permeability ($P_f \sim 100$ μm s^{-1} for very active aquaporins), and in some cases is also considered its inhibitory response to mercurial compounds (Finkelstein 1987; Verkman et al. 1996). These parameters can be assessed by (1) expressing the aquaporin in different heterologous systems (Preston et al. 1992; Karlsson et al. 2003) or (2) measuring the native plasma membrane water transport by means of stopped flow procedures applied to isolated vesicles, or by means of videomiscroscopy applied to isolated protoplasts (Meyer and Verkman 1986; Maurel et al. 1997; Moshelion et al. 2004). However, only the expression of aquaporins in heterologous systems unequivocally allows the identification of its individual properties (Agre et al. 1999).

Even though all PIPs share high amino acid sequence identity, only PIP2 isoforms have shown high water transport activity when expressed individually in a heterologous system (Daniels et al. 1994; Fetter et al. 2004). On the other hand, when PIP1 isoforms are expressed alone show null or low water activity. It has been postulated that when PIP1 is co-expressed with PIP2 in Xenopus oocytes there is a re-localization of PIP1 to the plasma membrane (PM), suggesting that PIP1–PIP2 hetero-oligomerization is required for the correct attachment of PIP1 to the PM (Fetter et al. 2004). Recent work has also demonstrated that PIP1 is mainly retained in the endoplasmic reticulum (ER) and can be re-localized to the PM when co-expressed with PIP2 in mesophyll protoplasts (Zelazny et al. 2007).

All the above observations contribute to explain the low water permeability measured on the plasma membrane of the Xenopus oocytes injected only with PIP1 cRNA (Fetter et al. 2004; Temmei et al. 2005; Mut et al. 2008). It has been difficult to further explore its functional properties in heterologous systems as a consequence the complexity of its localization in PM. Nevertheless, it is clear that modulating *whole plasma membrane water permeability* could be strongly dependent of PIP1–PIP2 interaction since the absence of PIP2 isoforms seem to restrict PIP1 participation.

Both PIP1 and PIP2 have conserved residues in their sequence that sense cytosolic pH, providing the capacity to reduce *water permeation through the pore* by acidification as a result of a channel gating process. This mechanism was completely clarified in a series of landmark works: (1) the gating mechanism of the inhibitory effect was explained by the protonation of a conserved histidine residue located on the intracellular-exposed loop D of PIPs (Tournaire-Roux et al. 2003), (2) fast volume change kinetics, analyzed by stopped flow methods, unequivocally demonstrated that root plasma membrane with highly active aquaporins shut down by cytosolic acidification (Alleva et al. 2006), (3) a structural mechanism for pH dependence of PIP gating was proposed based on the structures of the closed and open conformations of a plant aquaporin as determined by X-ray diffraction studies (Törnroth-Horsefield et al. 2006).

In the present work, we decided to explore if the ability of modulating *whole membrane water permeability* by PIP1–PIP2 co-expression, and the PIP capacity to reduce *water permeation through the pore* as a consequence of a channel gating process, can jointly trigger a cooperative interaction. Our working hypothesis is that if both processes interact, the plasma membrane will increase its plasticity to finely adjust water transfers.

We focused our interest in understanding water movements on *Beta vulgaris* storage roots as an halophyte model that is easily manipulated at different levels: (1) in root slices we identified a transcellular water pathway sensitive to mercurial compounds (Amodeo et al. 1999); (2) in the root tonoplast (vacuoles and isolated tonoplast vesicles) we showed water channel activity (Amodeo et al. 2002; Sutka et al. 2005) and (3) in the root plasma membrane (isolated PM vesicles) we described a high P_f with partially inhibitory response to mercurial compounds but showing a strong reduction in the presence of intracellular acidification or calcium (Alleva et al. 2006). The latter findings were of particular interest since isolated PM vesicles from several species show low water transport activity (Dordas et al. 2000; Gerbeau et al. 2002; Niemietz and Tyerman 1997) while PM vesicles from *Beta vulgaris* storage root show atypically high water permeability ($P_f = 542$ μm s^{-1}), equivalent to those reported only for active aquaporins in tonoplasts or animal red cells (Preston et al. 1992). The study of whole membrane water permeability of PM vesicles reflects the activity of all the complete set of aquaporins present in the membrane preparation. Consequently, to test our hypothesis (interaction of co-expression and channel gating modulation by pH), it is necessary to analyze the PIP individual contribution to the final plasma membrane P_f. This can only be achieved by means of PIP expression in heterologous systems. The *Beta vulgaris* genome sequence is not yet available despite its small size (~750 Mb) and the agronomic importance of this species. The molecular identification of some aquaporins in the plasma membrane of cells from *Beta vulgaris* storage tissue has been reported (Qi et al. 1995; Barone et al. 1997, 1998). Unfortunately, a

complete functional analysis of these or other *Bv*PIPs is still missing.

We present here the characterization of root *Beta vulgaris* PIPs expressed in *Xenopus laevis* oocytes and we show for the first time that PIP co-expression affects the pH regulatory response, enhancing in this way membrane versatility to adjust its water transfer capacity.

Materials and methods

Plant material

Commercial red beets (*Beta vulgaris*) were maintained in well watered soil until required for experiments. For RT-PCR analysis *Beta vulgaris* var. Detroit was grown under controlled environmental conditions with a 15/9 h light/dark cycle (light intensity of 68.62 ± 11.30 µmol m^{-2} s^{-1}) in a 20°C conditioned room. Red beet seeds were germinated in plastic containers filled with vermiculite and they were moistened with the culture medium: 1.25 mM KNO_3, 0.75 mM $MgSO_4$, 1.5 mM $Ca(NO_3)_2$, 0.5 mM KH_2PO_4, 50 µM FeEDTA, 50 µM H_3BO_3, 12 µM $MnSO_4$, 0.70 µM $CuSO_4$, 1 µM $ZnSO_4$, 0.24 µM Na_2MoO_4, and 100 µM Na_2SiO_3 (Javot et al. 2003). Ten days after germination, healthy seedlings were transplanted into hydroponic culture. The medium was changed once a week and distilled water was added in the fourth day to compensate loses by evapotranspiration. Young plants were harvested 21 days after they were planted (9 days in hydroponic culture, when the first leaf was completely developed) and adult plants were harvested 41 days after they were planted (34 days in hydroponic culture, when the storage root was visible). Two groups of four plants each were processed for young plants and two groups of two plants for adult plants.

Sequences encoding PIP2 and PIP1 aquaporins

Storage root tissue from commercial red beets was collected and immediately frozen in liquid nitrogen. Duplicates samples of total RNA from two different plants were isolated using the Total RNA Isolation System (Promega, Madison, WI, USA) following the manufacturer's recommendation. For each sample, 2 µg of total RNA was reverse translated using Oligo(dT) and M-MLV Reverse Transcriptase (Promega, Madison, WI, USA). The coding regions of GenBank sequences U60149, U60148 and U60147 (here renamed *Bv*PIP1;1, *Bv*PIP2;1 and *Bv*PIP2;2) were amplified using *Taq DNA Polymerase* (Invitrogen, Brazil) in the case of *Bv*PIP1;1 and *Bv*PIP2;2, or *platinum Pfx DNA polymerase* (Invitrogen, Japan) in the case of *Bv*PIP2;1. The primers used were:

*Bv*PIP1;1F (5′-GGGAGATCTATGGAAGGGAAAGATG AAGATGTTAGAC-3′); *Bv*PIP1;1R (5′- GGACTAGTTTA CGACTTGGACTTGAATGGAATTGC-3′); *Bv*PIP2;1F (5′-GG GAGATCTATGACTAAGGAAGTAAGTGA-3′); *Bv*PIP2;1R (5′-GGGACTAGTTTAGTTGGTAGGGTTGCTTC-3′); *Bv*PIP2; 2F (5′-GGGAGATCTATGACCAAGGATGTGGAAGCA GTTTC-3′) and *Bv*PIP2;2R (5′-GGGACTAGTTTAAG CAGAGCTCCTGAAGGATCC-3′).

Amplified products were extracted using Wizard SV Gel and PCR Clean-up system (Promega, Madison, WI, USA) and cloned into the BglII and SpeI sites of a pT7Ts derived vector carrying 5′ and 3′ untranslated sequences of a *β*-globin gene from *Xenopus laevis* in order to promote translation efficiency of the plant cRNA (Agre et al. 1999). At least ten clones of each aquaporin were sequenced using a 3730xl DNA analyzer (Macrogen Inc. Seul, Korea). The nucleotide and deduced amino acid sequences were analyzed by LAling program by comparison to the respective available GenBank sequences.

Sequence analysis

Sequence search was performed using BLASTP tools (http://blast.ncbi.nlm.nih.gov/Blast.cgi).

Phylogenetic and molecular evolutionary analyses were conducted using MEGA version 3.0 (Kumar et al. 2004). Protein sequences were aligned using the Clustal W program. Phylogenetic trees were constructed using the neighbor- joining (NJ) method with genetic distances computed using p-distance model, bootstrap analysis of 1,000 resamples and root on midpoint. The tree topologies obtained using NJ method, Minimum evolution, Maximum parsimony or UPGMA methods were compared.

Sequence alignments were performed with Clustal W version 2 (Larkin et al. 2007). The following sequences were considered for the alignments: *So*PIP1;2 (*Spinacia oleracea*, AAR23268.1), *Sb*PIP1 (*Salicornia bigelovii*, ABE03629.1), MipA (*Mesembryanthemum crystallinum*, AAB09747), *Ac*PIP1 (*Atriplex canescens*, P42767), *So*PIP2;1 (*Spinacia oleracea*, Q41372), *Vv*PIP2;2 (*Vitis vinifera*, ABH09327), MipC (*Mesembryanthemum crystallinum*, AAB18227), *St*PIP2 (*Solanum tuberosum*, ABB29939), *At*PIP1;4 (*Arabidopsis thaliana,* NP567178), *At*PIP2;1 (*Arabidopsis thaliana,* NP190910), *At*PIP2;8 (*Arabidopsis thaliana*, NP179277), *Zm*PIP2;4 (AAK26761) and *Zm*PIP2;5 (AF130975). Postscript was generated from aligned sequences using ESPript 2.2 (Gouet et al. 1999).

In vitro synthesis and translation

Capped complementary RNAs (cRNA) encoding *Bv*PIP1;1, *Bv*PIP2;1 and *Bv*PIP2;2 were synthesized in vitro using the *mMESSAGE mMACHINE T7 High Yield*

Capped RNA Transcription Kit (Ambion, Austin, TX, USA). The pT7Ts derived vector carrying the corresponding PIP as template was linearized employing PstI. ARCA capped and poly (A) tailed complementary RNA was synthesized in vitro using the *mMESSAGE mMACHINE T7 Ultra Kit* (Ambion, Austin, TX, USA) in the particular case of *Bv*PIP2;1. *At*PIP2;3 (Daniels et al. 1994) cRNA was synthesized with *mMESSAGE mMACHINE T3 High Yield Capped RNA Transcription Kit* (Ambion Austin, TX, USA). All the synthesized products were suspended in RNAse-free water and diluted to a final concentration of 1 μg μl^{-1} for performing the oocyte microinjection (Preston et al. 1992). The cRNA was quantified by spectrophotometry and viewed in denaturized agarose gel to check that no unincorporated nucleotides interfered and to compare and ascertain that the different cRNAs have the same concentrations. Three independent cRNA synthesis were assayed. Results from experiments performed with the different RNA samples were not pooled, therefore all the experiments shown in this work are representative.

Oocyte transport studies

Defolliculated Xenopus oocytes were injected with different masses of cRNA or RNase free water (vehicle control) in a final volume of 50 nl. Injected oocytes were incubated for 3 days at 18°C in ND96 medium (96 mM NaCl, 2 mM KCl, 1 mM $MgCl_2$, 1.8 mM $CaCl_2$ and 5 mM HEPES pH 7.5; ~200 mOsmol kg^{-1} H_2O) supplemented with 1 μg ml^{-1} gentamycin sulfate. Osmotic water permeability (P_f) was determined by measuring the rate of oocyte swelling induced by transferring oocytes to the same solution diluted fivefold with distilled water. Briefly, changes in cell volume were video monitored by a Life CamVX-3000 color videocamera (Microsoft, CA, USA) attached to a zoom stereo-microscope (Olympus SZ61, Olympus Co., Tokyo, Japan). The camera was connected through an USB port to a PC computer. The cell swelling was videocaptured in still images (each 10 s during 60 s) using *AMCaP* version 9.20 (http://noeld.com/programs.asp?cat=video#AMCap). Then images were analyzed by treating each oocyte image as a growing sphere and thus inferring the volume from its cross-sectional area (Software *Image J* version 1.37; http://rsb.info.nih.gov/ij/). The osmotic water permeability (P_f) was calculated according to Zhang and Verkman (1991) and Agre et al. (1999): $P_f = V_o[d(V/V_o)/dt]/[S\ Vw\ (Osm_{in} - Osm_{out})]$, where V_o is initial oocyte volume ($9 \times 10^{-4} cm^3$), V/V_o is the relative volume, S is the surface area of the oocyte (0.045 cm^2), V_w the partial molecular volume of water (18 cm^3 mol^{-1}) and $Osm_{in} - Osm_{out}$ the osmotic driving force. All osmolarities were determined using a vapor pressure osmometer (5520C Wescor, Logan, UT).

As a positive experimental control, a well known aquaporin was employed (*At*PIP2;3) (Daniels et al. 1994) while for negative controls water injected or non-injected oocytes were used indistinguishable as no significative difference was found between these two conditions.

Aquaporin inhibition by pH

Oocyte internal (cytosolic) pH was modified following an already described protocol (Tournaire-Roux et al. 2003). Briefly, oocytes were pre-incubated for 15 min in a solution of pH 6.0 (NaAc Solution: 50 mM NaAc, 20 mM MES, supplemented with mannitol 1 M to adjust osmolarity to ~200 mOsmol $kg^{-1}H_2O$) or pH 7.5, replacing in this case MES by HEPES. The swelling response was performed by transferring the oocyte to the same solution diluted fivefold with distilled water in order to induce the osmotic shock.

Oocytes injected with cRNA of *At*PIP2;2 wild type or its mutant insensitive to pH (H197D) were used as an internal control to test the cytosolic pH drop (data not shown).

In order to assess experiments where only external pH was modified, solutions were prepared with 50 mM NaCl plus 20 mM MES to reach pH 6.0 or 20 mM HEPES to reach pH 7.5. In both cases solutions were supplemented with mannitol 1 M to adjust osmolarity to ~200 mOsmol $kg^{-1}H_2O$. The percentage of inhibition was calculated using the formula:

$$\mathrm{Inh}(\%) = \left[1 - \left(P_{f\,\mathrm{AQP}}pH_6 - P_{f\,\mathrm{NI}}pH_6\right)/\left(P_{f\,\mathrm{AQP}}pH_{7.5} - P_{f\,\mathrm{NI}}pH_{7.5}\right)\right] \times 100$$

For analyzing a broader pH range, the buffer solution was MES for the 5.8–6.7 pH interval and HEPES for the 7.0–7.5 pH interval. A qualitative intracellular pH indicator was employed to calculate final oocyte internal pH values in the whole range (see next section).

Internal pH measurement

Intracellular pH of the oocytes was measured as described by Sasaki et al. (1992) and Peracchia and Peracchia (2005). Briefly, the fluorescein derivative pH indicator BCECF B-1151 (Molecular Probes, Eugene, OR, USA) was injected into oocytes in amounts sufficient to reach an intra-oocyte concentration of 100 μM (Peracchia and Peracchia 2005). After the injection, the oocytes were incubated for 40 min and then placed in a built-in chamber, with the vegetative pole facing the fluorescent beam and held in place using a thin stainless steel wire. The chamber was mounted on the stage of a Nikon TE-200 epifluorescence inverted microscope provided with a Nikon Planfluor × 40 oil immersion objective lens. The focus was set at the

center of the bottom of the cell. Fluorescence was measured at an emission wavelength of 530 nm with alternatively excitation at 490 and 440 nm. Fluorescence ratio (490/440 nm) was acquired every 30 s by using a charge-coupled-device camera (Hamamatsu C4742-95, Japan) connected to a computer. The capture was performed using the acquisition program Metafluor (Universal Imaging, West Chester, PA, USA). During the first 6 min the fluorescence of an individual oocyte in ND96 solution was acquired, then the media was exchanged by aspiration and replaced by the NaAc solution at a different pH. The fluorescence was then acquired during 20 min. To calculate intracellular pH only the fluorescence ratio emission acquired from minute 14 to 16 was used. Calibration curves were generated by adding to an empty chamber 200 µl of the NaAc solution containing 13 µM BCECF. The relationship between fluorescence ratio and pH was adjusted to: $pH = pK_a + \log((R - R_{min})/(R_{max} - R))$, where R is the fluorescence ratio and R_{max} and R_{min} are the maximum and minimum fluorescence ratios (Graber et al. 1986). In all cases, the corresponding fluorescence background was subtracted before performing the ratio calculation.

RT-PCR

From young plants, leaf 1, its petiole and root were harvested and immediately frozen in liquid nitrogen. From adult plants, leaf 5 and 8 were harvested together with petiole of leaf 5, root and storage root. Total RNA was isolated using *RNeasy Plant Extraction kit* with *Plant RNA Isolation Aid* (Ambion, Austin, TX, USA) following the manufacturer's recommendation. DNAse I digestion was performed at the end of the isolation. For each RNA sample, 2 µg was reverse translated using Oligo(dT) and M-MLV Reverse Transcriptase (Promega, Madison, WI, USA) following the manufacturer's recommendation. The AQPs were amplified with the same primers of the subcloning. For Actin1 (*Beta vulgaris*, DQ866829) the following primers were used: *Bv*ActinF (5′-TGTGCTTGACTCTGGTGATGGTGT-3′) and *Bv*ActinR (5′-AGCAAGATCCAAACGGAGAATGGC-3′). PCR reaction was performed using Taq DNA polymerase (Invitrogen, Brazil). The fragments were analyzed in 0.8% agarose gel. Images were captured using G-Box Chemi (Syngene, Frederick, MD, USA). PCR reaction with total RNA instead of cDNA were performed to verify that no genomic DNA was amplified.

Statistical analysis

Results are reported in the form of means ± SEM. Significant differences between treatments were calculated using the Student's *t*-test.

Results

Identification of water channels in *Beta vulgaris* storage root

Three aquaporins were subcloned in red beet root tissue, classified after a Blastp analysis (http://blast.ncbi.nlm.nih.gov/Blast.cgi) and renamed following the nomenclature proposed for plant aquaporins (Johanson et al. 2001): *Bv*PIP1;1 (GenBank Accession Number GQ227845); *Bv*PIP2;1 (U60148) and *Bv*PIP2;2 (GQ227846). These proteins were initially referred by Barone et al. (1997) as *BPM3* (PMIP27), *BPM2* (PMIP31) and *BPM1* respectively. *Bv*PIP2;1 amino acid sequence was 100% equal to the one reported in the GenBank. Minor protein sequence changes were found for *Bv*PIP1;1 and *Bv*PIP2;2 in comparison with the previously reported sequences (GenBank Accessions of nucleotide sequence U60149 and U60147 codifying *Bv*PIP1;1 and *Bv*PIP2;2 respectively). For *Bv*PIP1;1 the modified amino acids were: I86V and L216F and in the case of *Bv*PIP2;2 were F115I and A165S.

Once these PIPs were identified as member of one of both clusters (PIP1 or PIP2), their final proposed name (by numbering *Bv*PIP2;1 or *Bv*PIP2;2) reflects order of appearance. Figure 1 shows a phylogenetic tree including PIPs from *Arabidopsis thaliana* and *Zea mays*, species whose genome has totally or almost completely been sequenced and that contain isoforms where PIP co-expression experiments have already been reported. As expected, *Bv*PIP1;1 is clustered with all PIP1s while *Bv*PIP2;1 and *Bv*PIP2;2 shares high identity with PIP2s.

Figure 2 shows the predicted amino acid sequence of *Bv*PIP1;1, *Bv*PIP2;1 and *Bv*PIP2;2 indicating the six transmembrane domains (H1–H6), and conserved residues (the two NPA motifs) typically present in almost all water channels. Note the extended N-termini and shorter C-termini for PIP1 cluster that differentiates them from PIP2. As also shown in the Fig. 2, the predicted amino acid sequence of the three *Bv*PIPs was compared to aquaporins from different sources. The criterion was selecting some PIPs with the highest identity and at least one from *Arabidopsis thaliana* genome.

*Bv*PIP1;1 resulted with 93.3% identity with *So*PIP1;2 (*Spinacia oleracea*); 91% with SbPIP1 (*Salicornia bigelovii*); 88.1% with MipA (*Mesembryanthemum crystallinum*) and 87.5% with *At*PIP1;4. Among these proteins, activity in Xenopus oocytes for MipA was very low (5% above water injected oocytes according to Yamada et al. 1995) while for *At*PIP1;4 was negligible (Tournaire-Roux et al. 2003). Functional studies are still not available for *Sb*PIP1 and *So*PIP1;2. Both *Sb*PIP1 and MipA belong to halophyte species.

In the case of *Bv*PIP2;1 the identity is 91% with *Ac*PIP1 (*Atriplex canescens*); 87.5% with *Vv*PIP2;2 (*Vitis vinifera*);

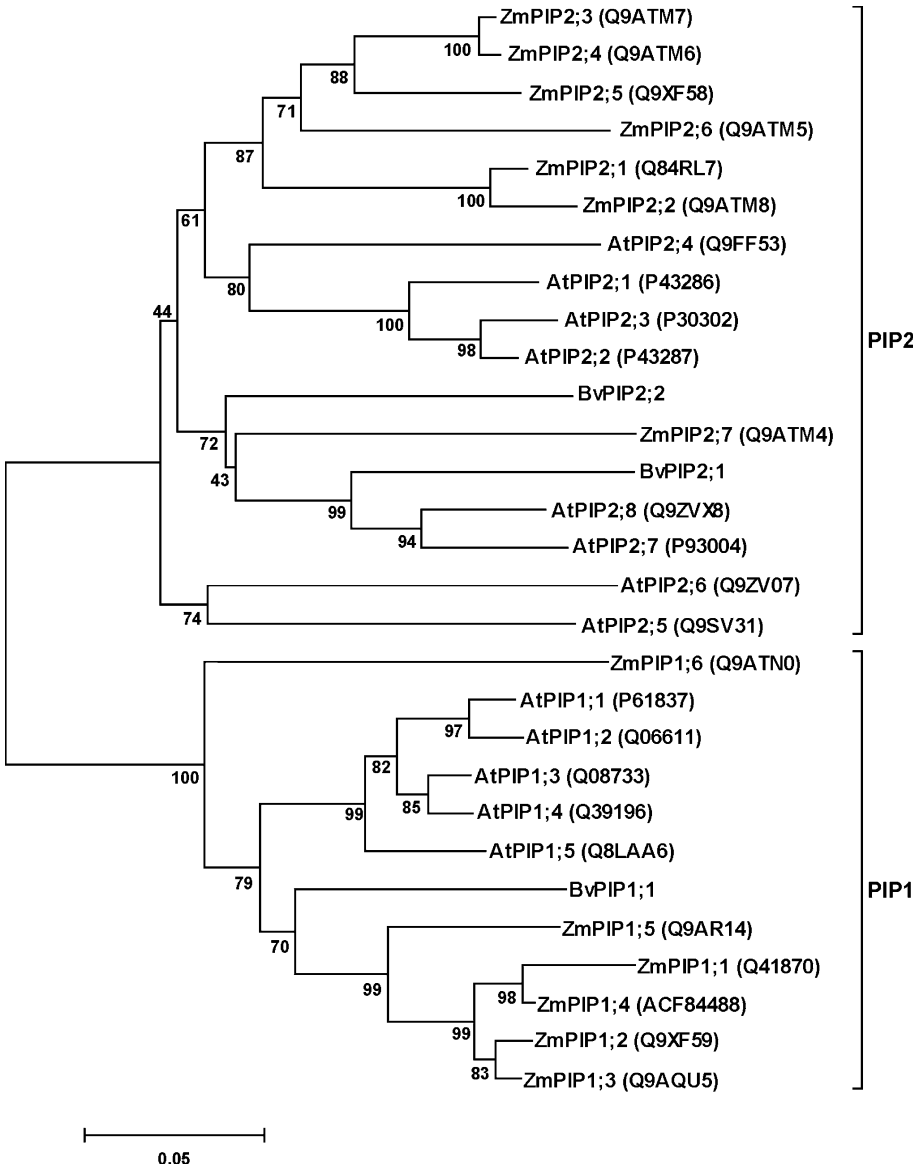

Fig. 1 PIPs phylogenia. Phylogenetic tree showing the two PIP conserved clusters: PIP1 and PIP2. The three *Beta vulgaris* aquaporins are compared with all the PIPs present in *Arabidopsis thaliana* and *Zea mays*. Phylogenetic relationships between representative taxa of the phylum Streptophyta are based on neighbor-joining (NJ) analysis of PIP proteins. Bootstrap percentages are indicated at the branch points. In all of the cases, tree topologies obtained using NJ method, Minimum evolution, Maximum parsimony or UPGMA methods were identical

87.4% with *So*PIP2;1 (*Spinacia oleracea*) and 86.8% with *At*PIP2;8. *So*PIP2;1 corresponds to the first plant aquaporin that has been crystallized (Törnroth-Horsefield et al. 2006) with a reported $P_f = 110$ μm s^{-1} for Xenopus oocytes expressing it (Johansson et al. 1998), while for oocytes expressing *Vv*PIP2;2 a $P_f \sim 45$ μm s^{-1} is reported (Vandeleur et al. 2009). It should be mentioned that *Bv*PIP2;1 shares the highest identity with *Ac*PIP1, an aquaporin that is not named according to the proposed nomenclature (Johanson et al. 2001) but belongs to the PIP2 cluster.

Finally, *Bv*PIP2;2 shares 85.8% identity with MipC (*Mesembryanthemum crystallinum*), 83.3% with *St*PIP2 (*Solanum tuberosum*); 80.6% with *At*PIP2;1. Water transport capacity of *At*PIP2;1 was proved to be high (Kammerloher et al. 1994) and a recent work described its gating process associated not only to pH but also to divalent cations (Verdoucq et al. 2008).

Functional studies of PIPs in *Xenopus laevis* oocytes

For further functional characterization, *Bv*PIPs were expressed in the heterologous system Xenopus oocytes. To evaluate their water transport capacity, oocytes expressing separately each *Bv*PIP were exposed to a hypotonic shock (1:5 medium dilution), which generates an osmotic gradient of 160 mOsm $kg^{-1}H_2O$ across the oocyte membrane (Preston et al. 1992; Agre et al. 1999). As shown in Fig. 3, the injection of *Bv*PIP2;2 cRNA in Xenopus oocytes led to a large increase of the swelling rate as compared with control oocytes (water injected) resulting in a P_f consistent

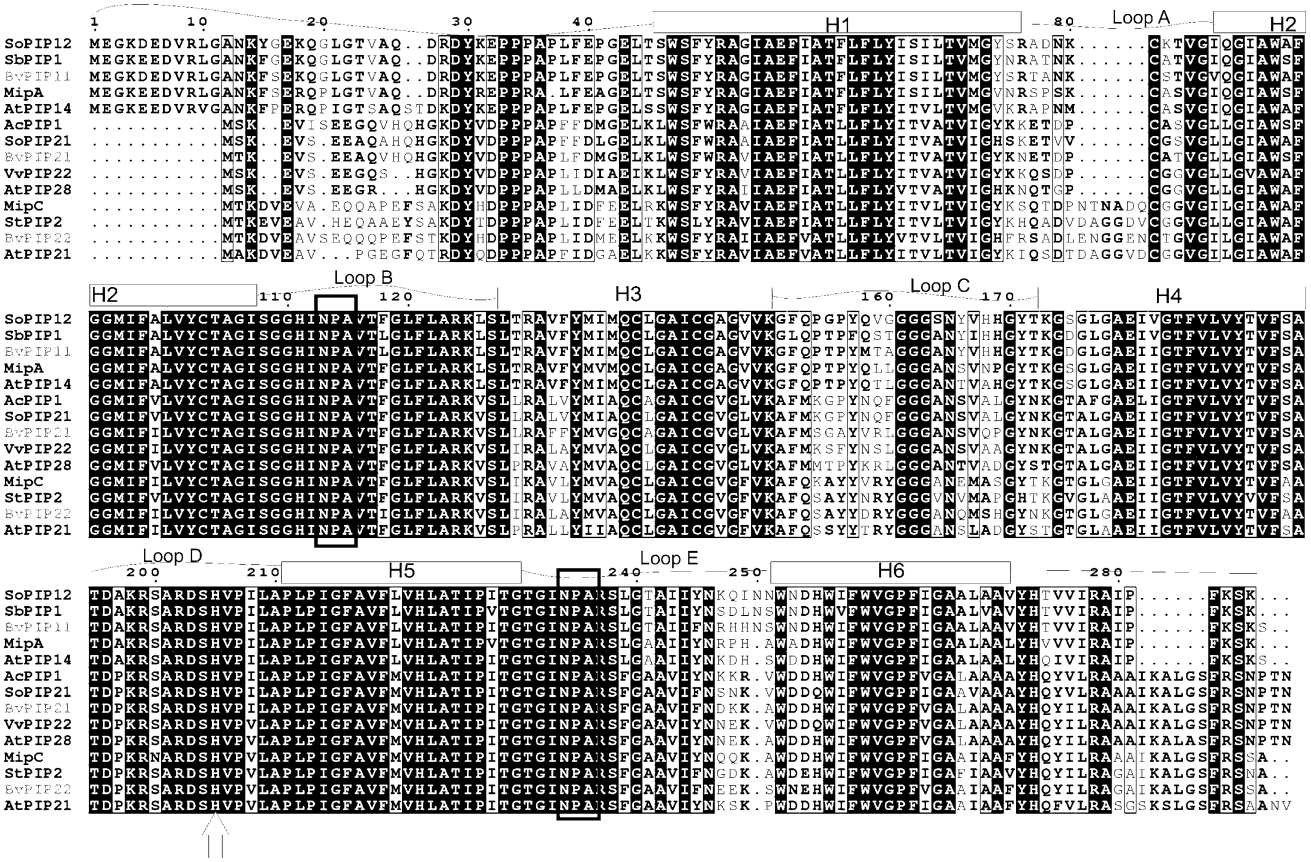

Fig. 2 Alignment of predicted amino acid sequence of *Beta vulgaris* aquaporins. The predicted amino acid sequence of *Bv*PIPs were compared to aquaporins from different sources: *So*PIP1;2 (*Spinacia oleracea*, AAR23268.1), *Sb*PIP1 (*Salicornia bigelovii*, ABE03629.1), MipA (*Mesembryanthemum crystallinum*, AAB09747), *At*PIP1;4 (*Arabidopsis thaliana,* NP567178); *Ac*PIP1 (*Atriplex canescens*, P42767), *So*PIP2;1 (*Spinacia oleracea*, Q41372), *Vv*PIP2;2 (*Vitis vinifera*, ABH09327), *At*PIP2;8 (*Arabidopsis thaliana*, NP179277); MipC (*Mesembryanthemum crystallinum*, AAB18227), *St*PIP2 (*Solanum tuberosum*, ABB29939), *At*PIP2;1 (*Arabidopsis thaliana,* NP190910). Conserved amino acids for all are shown in *dark boxes*. NPA motifs are indicated in boxes as well as each of the six transmembrane segments (H1 to H6). *Arrow* indicates one of the conserved histidines in *loop D* responsible of cytosolic pH sensing

with an active aquaporin expressed in the plasma membrane (82.2 ± 15.9 μm s^{-1}). *Bv*PIP1;1 injection did not modify membrane P_f substantially (13.7 ± 1.7 μm s^{-1}) if compared with the negative control (water injected oocytes, 19.6 ± 3.4 μm s^{-1}). This result is consistent with values reported for the majority of PIP1 when expressed alone in oocytes (Fetter et al. 2004). Unexpectedly, when *Bv*PIP2;1 cRNA was synthesized in the same condition that the other *Bv*PIP and then injected in oocytes, there was no evidence of a significatively increase of the oocyte plasma membrane P_f (19.2 ± 3.6 μm s^{-1}). However, when oocytes were injected with a *Bv*PIP2;1 cRNA synthesized using the anti-reverse cap analog (Stepinsky et al. 2001; Peng et al. 2002) and poly (A) tailing reagents, aquaporin activity was detected in the swelling experiments. In these conditions, the P_f of oocytes expressing *Bv*PIP2;1 was 86.2 ± 6.9 μm s^{-1} (Fig. 3b, dashed line). This data suggest that *Bv*PIP2;1 cRNA needs more protection for an efficient translation into oocytes. In all experiments *At*PIP2;3 was used as a positive control (Daniels et al. 1994) as this aquaporin has already been characterized as a water permeable channel. From these results we concluded that only the injection of *Bv*PIP2;1 and *Bv*PIP2;2 cRNA impact in the expression of aquaporins that induced a high water permeability in the oocyte membrane. Due to the novel observation reported here for a PIP2 (precisely *Bv*PIP2;1, in terms of an unexpected cRNA degradation that requests protection for ensuring protein expression in Xenopus oocytes) this aquaporin was not included in the co-expression experiments.

Co-expression of PIPs in *Xenopus laevis* oocytes

Co-injection of *Bv*PIP1;1-*Bv*PIP2;2 in a cRNA mass relation 3:1 triggered the membrane P_f sevenfold to a value of 281.0 ± 19.5 μm s^{-1}, value much higher than the one expected if both *Bv*PIPs contributed with the sum of the measured P_f for individual expression.

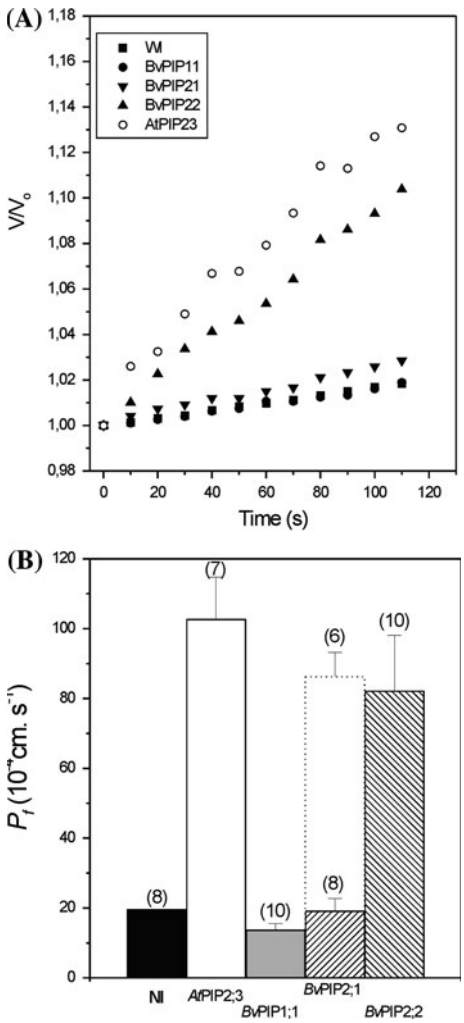

Fig. 3 Functional expression of *Bv*PIPs in Xenopus oocytes. **a** A typical experiment showing the time course evolution of the relative volume change of microinjected oocytes when exposed to an osmotic gradient. WI corresponds to water injected (negative control), *At*PIP2;3 is included as a positive control and the rest corresponds to cRNA injected from the three *Beta vulgaris* PIPs. **b** Calculated mean water permeabilities ($P_f \pm$ SEM) of oocytes (third day after injection) expressing *Bv*PIP2;1, *Bv*PIP2;2 and *Bv*PIP1;1 and submitted to an hypo-osmotic shock. *Bv*PIP2;2 behaves as a functional water channel showing a high P_f as the one observed in *At*PIP2;3. *Bv*PIP2;1 shows only high P_f (*dashed line*) when synthesized with a modified protocol that protects the cRNA more efficiently. Number of measured oocytes for each condition is indicated in *brackets*. In all cases 25 ng of cRNA were microinjected

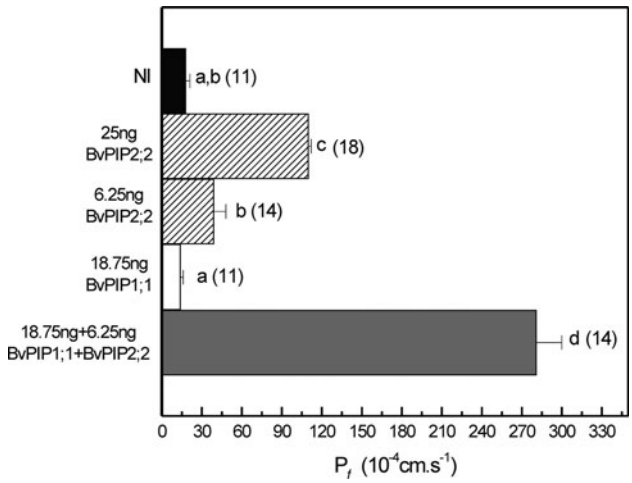

Fig. 4 Co-expression of *Bv*PIP2;2 and *Bv*PIP1;1. Oocytes co-expressing a low concentration of *Bv*PIP2;2 (6.25 ng of cRNA injected) with a high concentration of *Bv*PIP1;1 (18.75 ng of cRNA injected) showed a sevenfold water permeability increment versus oocytes expressing *Bv*PIP2;2 alone (6.25 ng of cRNA injected). Data are expressed as mean values ($P_f \pm$ SEM) and the number of measured oocytes for each condition is indicated in *brackets*. Different *letters* indicate significance between bars ($P < 0.05$). NI are non injected oocytes

To perform this co-injection experiment, the total mass of *Bv*PIP2;2 cRNA injected in the oocyte was reduced as much as to maintain a low P_f. In this condition, it is expected to avoid the immediate burst of the oocyte expressing both PIP1 and PIP2 subtypes. Figure 4 shows that while 25 ng of injected *Bv*PIP2;2 resulted in a final oocyte membrane $P_f = 109.5 \pm 19.3$ µm s^{-1}, lowering the mass to 6.25 ng allowed a final $P_f = 39.4 \pm 9.2$ µm s^{-1}. It should be emphasized that every set of experiments were carefully repeated with all the correspondent internal controls, therefore variations between the final P_f values of oocyte membrane expressing *Bv*PIP2;2 in Figs. 3 and 4 could be attributable to differences in oocyte batches. This variation did not affect the significance of the data.

The pH effect: the inhibitory response triggered by intracellular acidification

The next step was to characterize the P_f inhibitory response of the *Beta vulgaris* aquaporins triggered by cytosolic acidification. In these experiments, oocytes were incubated at two different pH values (7.5 and 6.0). In NaCl solutions (Tournaire-Roux et al. 2003; see "Material and methods") pH_{int} remained unaltered while in NaAc solutions final pH_{int} was modified after incubation. Oocyte internal pH was measured by means of a fluorimetric method and the calculated pH_{int} values were 7.1 and 6.4 when oocytes were exposed to NaAc solutions at pH 7.5 and 6.0 respectively.

To test the proper pH_{int} drop and the required incubation time when using the working solutions, a set of experiments were performed employing *At*PIP2;2 wild type and its mutant insensitive to pH (*At*PIP2;2 H197D) as described in Tournaire-Roux et al. (2003). In these experiments, after a 15 min incubation period, oocytes expressing the mutant showed high P_f when exposed to NaAc solution pH 6, while oocytes expressing the wild type aquaporin showed the expected inhibitory response, i.e. low P_f (data not shown). These observations are consistent with previous

results (Tournaire-Roux et al. 2003). As shown in Fig. 5a, when 25 ng of *Bv*PIP2;2 cRNA were injected alone, the P_f was significantly reduced at pH_{int} 6.4. This partial inhibitory response was (70 ± 5)%.

The putative pH effect could not be evaluated in the conditions where the P_f values were low or indistinguishable from non injected (i.e. *Bv*PIP1;1 expressed alone).

Interestingly, *Bv*PIP1;1-*Bv*PIP2;2 co-expression completely decreases membrane P_f from 198 ± 20 μm s^{-1} to 10.9 ± 1.5 μm s^{-1} when the internal oocyte pH was reduced to 6.4.

To further analyze the partial or total P_f blockage, different conditions were studied (Fig. 5a). First, different mass quantities of *Bv*PIP2;2 cRNA (25, 18.75 and 6.25 ng) were injected and P_f inhibitory response was always partial independently of the mass injected. Second, cRNA mass proportion employed for the co-expression *Bv*PIP1;1-*Bv*PIP2;2 was inverted from 3:1 to 1:3, and as shown in Fig. 5a, in both cases not only P_f remains high at pH_{int} 7.1 but also completely shuts down at pH_{int} 6.4.

To test the reversibility or any putative change in protein stability triggered by internal acidification, we performed in the same oocyte a time course experiment with steps of pH change and swelling. As shown in Fig. 5b, a single oocyte expressing *Bv*PIP2;2 or *Bv*PIP2;2-*Bv*PIP1;1 is submitted to swelling by being exposed to a hypo-osmotic (threefold diluted medium) solution at a specific pH. After the hypo-osmotic shock, the oocyte is then returned to iso-osmotic conditions. In order to modify internal pH, the oocyte is then exposed during 15 min to a solution with a higher pH and then, the swelling assay is repeated under this new pH condition. Results shows that the oocyte maintains the ability to swell and reverse the swelling in hypo/iso-osmotic conditions in accordance to internal pH, no matter the treatment performed previously, indicating that the water channels expressed are intact (Fig. 5b). Moreover, the change in the slope of relative volume vs time during the hypo-osmotic shock becomes steeper, reflecting the water transport capacity through aquaporins at higher pH values.

Being confirmed that co-expression of PIPs alters membrane capacity to respond to internal pH by changing its water permeability we evaluated the pH dependence of this inhibitory response. For this purpose, oocytes expressing *Bv*PIP2;2 alone or co-expressing *Bv*PIP1;1-*Bv*PIP2;2 (injected cRNA mass ratio 3:1) were incubated 15 min at different pH increasing from 5.8 to 7.5, in a 0.3 pH step. Then, each oocyte was transferred to a fivefold diluted medium at the same pH and the swelling assay was performed. Figure 6 shows P_f calculated for each experimental condition, including water injected oocytes as controls. As expected, at physiological pH the P_f of co-expressed PIPs remains higher than *Bv*PIP2;2 alone. Notably, when there is

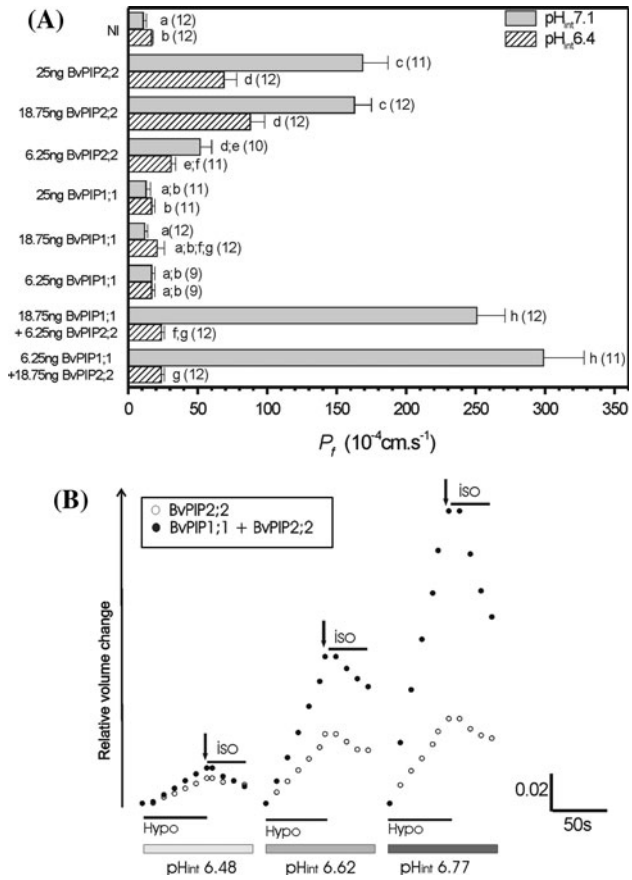

Fig. 5 P_f inhibitory response triggered by cytosolic acidification. **a** *Bv*PIP2;2 and *Bv*PIP1;1 were expressed separately in Xenopus oocytes and exposed to two different pH media. *Bv*PIP2;2 expressed alone displayed the expected P_f increment at pH_{int} 7.1 and a significant decrease when pH_{int} was reduced to 6.4. *Bv*PIP1;1 alone showed a very low P_f independently of internal pH value. *Bv*PIP1;1-*Bv*PIP2;2 co-expression completely shuts down P_f when the internal oocyte pH is reduced to 6.4. Data are expressed as mean values (P_f ± SEM), number of measured oocytes for each condition is indicated in *brackets*. Different *letters* indicate significance between bars ($P < 0.05$). NI are non injected oocytes. **b** Relative volume change of a single oocyte was followed in a time course experiment performed with steps including pH change and a swelling challenge. The experiment was performed in an oocyte expressing only *Bv*PIP2;2 and in an oocyte co-expressing *Bv*PIP2;2:*Bv*PIP1;1

co-expression the pH dependence curve is affected and shifts EC_{50} from 6.5 to 6.9 pH values.

Finally, we also tested if co-expression triggers any external pH response by incubating the oocytes in a NaCl solution at two different pH. Oocytes co-expressing *Bv*PIP1;1-*Bv*PIP2;2 (3:1 mass ratio) showed high P_f when exposed to a hypo-osmotic challenge both at external pHs, 6.0 and 7.5. The calculated P_f for both conditions was 242.34 ± 19.08 μm s^{-1} ($n = 6$) and 294.38 ± 50.82 μm s^{-1} ($n = 7$), respectively, showing statiscatically no significative differences. Three independent experiments including internal controls of each *Bv*PIP expressed alone

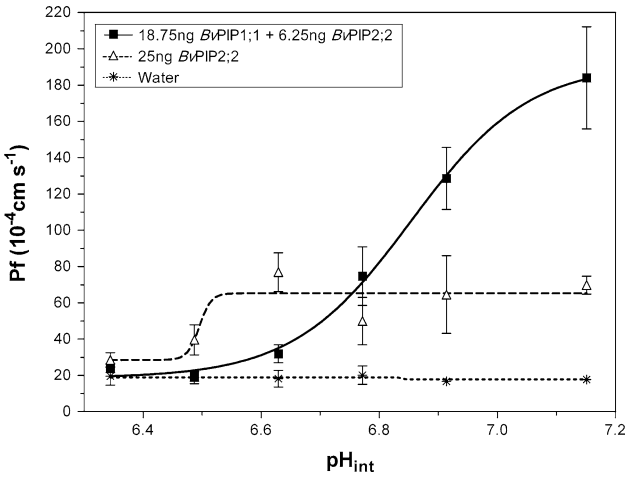

Fig. 6 pH_{int} dependence of the P_f inhibitory response for PIP expressed alone or co-expressed. To test cytosolic pH sensing, oocyte expressing *Bv*PIP2;2 or co-expressing *Bv*PIP1;1-*Bv*PIP2;2 (3:1 mass ratio) were incubated 15 min at different pH media ranging from 5.8 to 7.5. Then each oocyte was transferred to a fivefold diluted medium at the same pH and the swelling assay was performed. Data are mean values ($P_f \pm$ SEM) of five independent experiments within different oocyte batches, employing 4–7 oocytes per treatment in each experiment. Data were fitted to a sigmoidal dose–response curve using GraphPad Prism (version 3.02)

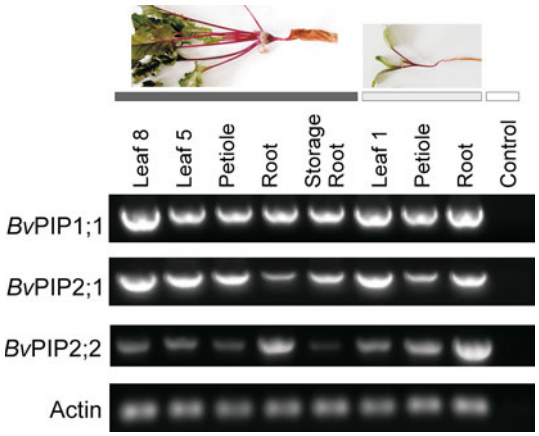

Fig. 7 Expression pattern of *Bv*PIP in *Beta vulgaris*. RT-PCR analysis was performed in red beet *Beta vulgaris* var. Detroit in both young and adult plants in order to identify pattern expressions in different organs and/or tissues

were performed in these conditions with similar results (data not shown).

PIP expression pattern at the tissue level

The results presented here show that PIP1–PIP2 co-expression triggers synergistically membrane P_f and also modifies its pH sensing capacity. This co-expression effect is relevant *in planta* only if PIPs are actually expressed in the same cell. As a first approach we checked if the *Bv*PIPs described here are expressed in the same tissue. By performing RT-PCR, we confirmed that *Bv*PIP1;1, *Bv*PIP2;1 and *Bv*PIP2;2 are non tissue specific, and they all coexist not only in the storage root tissue but also in other parts of the plant (Fig. 7). These results are consistent with the previous reports where plasma membrane vesicles from red beet showed mainly the expression of two highly abundant PIPs (Qi et al. 1995; Barone et al. 1997 and 1998), *Bv*PIP1;1 and *Bv*PIP2;1. Isolated PM vesicles from *Beta vulgaris* storage root tissue show a high P_f that is completely blocked by pH (Alleva et al. 2006).

Discussion

In a previous work we analyzed the *whole plasma membrane water permeability* of *Beta vulgaris* storage root tissue (Alleva et al. 2006). Now, we present the functional characterization of aquaporins expressed in that tissue. Information available in the Genbank allowed us to subclone three different aquaporins, named *Bv*PIP1;1 *Bv*PIP2;1 and *Bv*PIP2;2 according to sequence identity and the proposed nomenclature for plant aquaporins (Johanson et al. 2001) (Figs. 1, 2).

Xenopus oocytes expressing *Bv*PIP2;1 and *Bv*PIP2;2 show high P_f (86.22 ± 6.92 μm s^{-1} and 82.2 ± 15.9 μm s^{-1}, respectively). In the particular case of *Bv*PIP2;1, an atypical observation (a low P_f for a PIP2 as shown in Fig. 3b) was detected, similar to that reported for two other species, *Pv*PIP2;2 and *Tg*PIP2;1 (Zhou et al. 2007; Azad et al. 2008, respectively). As *Bv*PIP2;1 shares high identity with other water permeable PIP2 isoforms from different species, this feature is quite intriguing. Interestingly, it was sufficient to specially protect *Bv*PIP2;1 cRNA (capped with an anti-reversed cap analog and poly(A) tailed) to ensure protein expression. It is not clear why *Bv*PIP2;1 requests this special treatment but these observations should be considered when functionally characterizing other PIP2.

Oocytes expressing *Bv*PIP1;1 present low membrane P_f values (13.7 ± 1.7 μm s^{-1}). This behavior was expected since recent findings described that it does not spontaneously reach the PM (Fetter et al. 2004; Zelazny et al. 2007 and 2009). These authors showed that in maize protoplasts PIP1 mainly remains in the endoplasmic reticulum while PIP2 is able to reach the plasma membrane. However, if PIP1 and PIP2 are both present in the cell, PIP1 is able to be localized in the PM together with PIP2. It was also demonstrated that for some specific PIP2 a diacidic motif seems to be involved for allowing ER export (Zelazny et al. 2009). Figure 8 shows a sequence comparison of *Bv*PIP2;1 and *Bv*PIP2;2 to check for the presence or absence of a diacidic motif as described in maize PIP. This comparison

```
                 * *                  *** ******* *   **   **
ZmPIP2.4   MAKDIEASGPEAG-EFSAKDYTDPPPAPLIDAEELTQWS 38
ZmPIP2.5   MAKDIEAAAAHE-----GKDYSDPPPAPLVDAEELTKWS 34
BvPIP2.2   MTKDVEAVSEQQQPEFSTKDYHDPPPAPLIDMEELKKWS 39
BvPIP2.1   MTK---EVSEEAQVHQHGKDYVDPPPAPLFDMGELKLWS 36
```

Fig. 8 Amino acid sequence alignment showing the cytosolic N-terminal region of *Zm*PIP2;4, *Zm*PIP2;5, *Bv*PIP2;2 and *Bv*PIP2;1. *Asterisks* indicate single, fully conserved residues. Potential diacidic motifs are indicated in *bold*. The conserved N-terminal diacidic signal (DIE, *underlined*) was demonstrated to be involved in endoplasmic reticulum export for the shown *Zm*PIP

indicates the presence of a potential diacidic motif only in *Bv*PIP2;2.

PIP co-expression induces a high P_f improving membrane water transport capacity. In accordance with these results, the co-expression of *Bv*PIP1;1:*Bv*PIP2;2 enhances sevenfold oocyte plasma membrane P_f respect to the expression of *Bv*PIP2;2 alone (Figs. 4, 5a) and this effect is much higher than the reported value from other species (for instance, PIPs from *Zea mays* and *Vitis vinifera* leads to almost fourfold increments (Fetter et al. 2004; Vandeleur et al. 2009).

High P_f amplification due to PIP co-expression could explain the high water permeability already reported in the native *Beta vulgaris* plasma membrane ($P_f = 542$ μm s^{-1}) (Alleva et al. 2006) and the transcellular water pathway identified in root slices (Amodeo et al. 1999).

RT-PCR results confirm the presence of *Bv*PIP1;1, *Bv*PIP2;1 and *Bv*PIP2;2 in storage root tissues as well as in other tissues.

Barone et al. (1998) demonstrated tissue-specific differences in expression patterns of the *BPM2* (here *Bv*PIP2;1) and *BPM3* (here *Bv*PIP1;1) genes using RNA gel-blot analysis. A single 1.2-kb *BPM2* transcript was strongly detected in storage tissue, but was barely detectable in leaf and stem tissue. The 1.3-kb *BPM3* transcript was mostly expressed in storage tissue and moderate levels were also present in stem tissue.

The presence of *Bv*PIPs in the root suggests that there is a possibility of finding these aquaporins also expressed in the same cell. In favour of this hypothesis Barone et al. (1998) found that two of these aquaporins (here *Bv*PIP1;1 and *Bv*PIP2;1) are associated with the same population of membrane vesicles. The high membrane P_f observed in isolated root PM vesicles as well as the complete shutdown of water transport capacity at low pH (Alleva et al. 2006) also recalls the result of a synergistic PIP1–PIP2 interaction. Moreover, a mathematical model developed to explain the water transport kinetics of *Beta vulgaris* storage root PM vesicles showed that the water pathway completely inhibited by acidic pH behaves as an homogeneous preparation, strengthening the idea of both PIP in a single membrane (Alleva et al. 2009). Therefore, it is expected that these two aquaporins are involved in providing high levels of water permeability to the transcellular route.

Highly conserved histidines have been described to be responsible of a pH inhibitory response, shutting down PIPs when cytosolic medium is acidified (Tournaire-Roux et al. 2003). Plasma membrane of beet root vesicles suffered a dramatic reduction in their P_f due to aquaporin inhibition when the osmotic shock was performed under acidic conditions (Alleva et al. 2006). Here we tested if *Bv*PIPs were also sensitive to pH_{int} acidification. *Bv*PIP2;2 expressed alone showed a strong but partial P_f blockage (Fig. 5) which was independent of the cRNA mass injected. Hence, *Bv*PIP2;2 by itself cannot explain the dramatic reduction in P_f reported in isolated vesicles when the intravesicular medium was acidified (Alleva et al. 2006). The results presented here show that the co-expression of *Bv*PIP1;1 and *Bv*PIP2;2 can shut down P_f in a similar response to that reported for storage root PM vesicles. *Bv*PIP1;1 presence or absence when *Bv*PIP2;2 is in the plasma membrane can therefore regulate the partial or total inhibitory response at pH 6.4. To assign the change in water permeability to gating mechanism operating at the protein level it should be discarded pH- dependent PIP trafficking or any altered expression efficiency in combination with a change in stability/degradation of the protein.

PIP trafficking due to internal acidification can be hardly taken into account since the same shut-down effect triggered by acidic pH was also observed in fast volume change kinetic experiments performed on PM vesicles (Alleva et al. 2006) and in proteoliposomes (Verdoucq et al. 2008). In these experiments, not only the time course scale is too fast (~400 ms) but also both PM vesicles and proteoliposomes are systems lacking the cytoplasmatic machinery.

A pH dependent altered expression efficiency can also be set aside because independently of the pH experiments, oocytes are always incubated in the same medium (ND96, pH 7.4) during 72 h after cRNA injection. Therefore, there are no possibilities of different aquaporin expression efficiency for oocytes due to the different internal pH stimulus since the protein expression occurs before the pH treatment. Finally, to discard a change in stability/degradation of the protein we tracked the same oocyte in a time course experiment with steps of pH change and swelling (Fig. 5b). In these conditions it was demonstrated not only reversibility but also that the oocyte maintains the ability to swell

in accordance to internal pH, no matter the treatment performed previously, indicating that the expressed water channels are intact.

Our next step was to test if the inhibitory response is pH dependent. It was previously reported that *At*PIP2;1 reconstituted in proteoliposomes showed a half inhibition at pH 7.15 (Verdoucq et al. 2008). *Beta vulgaris* and *Arabidopsis thaliana* isolated PM vesicles showed respectively an EC50 of 6.7 (Alleva et al. 2006) and 7.2 (Gerbeau et al. 2002). We demonstrated here that the half inhibition response of *Bv*PIP2;2 when it is solely expressed is more acidic and that this response is altered when this aquaporin is co-expressed with *Bv*PIP1;1. Thus, the co-expression changes the pH sensing by shifting EC50 to pH 6.9 (Fig. 6). Again, *Bv*PIP1;1 not only contributes enhancing P_f but also adjusts the pH sensitivity to more physiological values.

Our findings described the behaviour of a membrane expressing more than one kind of PIP in terms of water permeability and pH. Two alternatives are now discussed: Does PIP2 solely help PIP1 target the membrane, showing therefore PIP1 high P_f and a higher response to pH than PIP2? A few PIP1 have demonstrated to be able to transport water alone. Or, does PIP1 and PIP2 form hetero-oligomers that have much higher P_f and a different response to pH than single PIP2? *Nt*AQP1, a PIP1 member, induced not only a low water permeability in the oocyte membrane when expressed in this heterologous system (Biela et al. 1999) but also when expressed in yeast (Fischer and Kaldenhoff 2008). Tournaire-Roux et al. (2003) reported a PIP1 (*At*PIP1;2) that could be expressed alone in Xenopus and upon submitting the oocytes to an osmotic challenge, the membrane P_f was much lower than that observed when *At*PIP2;2 cRNA was injected. In both cases, the sensitivity to cytosolic acidification was very similar. However, despite the low activity of the majority of PIP1 assayed in Xenopus oocytes (Fetter et al. 2004), this type of aquaporins must not be considered as an irrelevant component in terms of water transport capacity for the whole plant. In fact, recently it was demonstrated that *At*PIP1;2 is a key component of Arabidopsis whole hydraulic conductance (Postaire et al. 2010).

The findings reported here also contribute to the discussion of PIPs pH sensing capacity in terms of a real gating mechanism (Fischer and Kaldenhoff 2008; Verdoucq et al. 2008). In the case of an effective pH dependent aquaporin closure by a gating mechanism, it is expected to obtain P_f values similar to that of controls, and only this fact may be interpreted as a complete and effective closure of the channels. Verdoucq et al. (2008) reported a full inhibition of Arabidopsis PIP2;1 reconstituted in proteoliposomes by varying pH between 3.8 and 9.5. However, in a recent work it was proposed that not necessarily PIPs fulfil the requirements for the pH dependent gating as predicted (Fischer and Kaldenhoff 2008). Although the authors in their work clearly support the role of His196 as a component of pH dependent aquaporin response, they found that *Nt*PIP2;1 expressed in the yeast system shows a clear but partial pH sensitivity. Our results report both partial and complete P_f inhibition. When expressing *Bv*PIP2;2 alone in Xenopus the inhibitory response is partial (Fig. 5a), but the predicted gating mechanism is only observed when PIPs from both clusters are co-expressed. In this latter case P_f values drop to control ones and a "shutdown" situation arises. More studies are required for the molecular interpretation of the gating process to support the functional analysis observed in native plasma membrane vesicles of *Beta vulgaris*, including the novel results presented here.

In conclusion, we show for the first time that PIP co-expression influences the pH regulatory response, enhancing the membrane plasticity to control water movements which means versatility to finely adjust its water transport capacity.

Acknowledgments Our particular thanks are due to Noel Danjou who improved AMCAP program (version 9.20; http://noeld.com/programs.asp?cat=video#AMCap) to allow acquisition of still images as requested; Alex Paladini (INGEBI, CONICET) who designed and provided us with built-in chambers for oocyte experiments; Christophe Maurel (INRA, France) for kindly providing us with *At*PIP2;2 (wild type and the H197D mutant); Mark Daniels (UCSD, USA) for the kindly gift of *At*PIP2;3 cDNA; Victoria Espelt and Cora Alvarez for their invaluable contribution with the fluorimetric measurements and Alejandro C. Paladini for helpful comments in the ms. This work was financed by the PRESTAMO BID PICT04 949, UBACyT0810 and CONICET PIP5154, grants to GA and PRESTAMO BID PICT06 01804 grant to KA. KA and GA are Career Research Members of CONICET.

References

Agre P, Mathai JC, Smith BL, Preston GM (1999) Functional analyses of aquaporin water channel proteins. Methods Enzymol 294:550–572

Alleva K, Niemietz CM, Sutka M, Maurel C, Parisi M, Tyerman SD, Amodeo G (2006) Plasma membrane of *Beta vulgaris* storage root shows high water channel activity regulated by cytoplasmic pH and a dual range of calcium concentrations. J Exp Bot 57:609–621

Alleva K, Chara O, Sutka MR, Amodeo G (2009) Analysis of the source of heterogeneity in the osmotic response of plant membrane vesicles. Eu Biophys J 38(2):175–184

Amodeo G, Dorr R, Vallejo A, Sutka M, Parisi M (1999) Radial and axial water transport in sugar beet storage root. J Exp Bot 50:509–516

Amodeo G, Sutka M, Dorr R, Parisi M (2002) Protoplasmic pH modifies water and solute transfer in *Beta vulgaris* root vacuoles. J Membr Biol 187:175–184

Azad AK, Katsuhara M, Sawa Y, Ishikawa T, Shibata H (2008) Characterization of four plasma membrane aquaporins in tulip petals: a putative homolog is regulated by phosphorylation. Plant Cell Physiol 49:1196–1208

Barone LM, Shih C, Wasserman BP (1997) Mercury-induced conformational changes and identification of conserved surface loops in plasma membrane aquaporins from higher plants. Topology of PMIP31 from *Beta vulgaris* L. J Biol Chem 272:30672–30677

Barone LM, Mu HH, Shih CJ, Kashlan KB, Wasserman BP (1998) Distinct biochemical and topological properties of the 31- and 27- kilodalton plasma membrane intrinsic protein subgroups from red beet. Plant Physiol 118:315–322

Biela A, Grote K, Otto B, Hoth S, Hedrich R, Kaldenhoff R (1999) The *Nicotiana tabacum* plasma membrane aquaporin NtAQP1 is mercury-insensitive and permeable for glycerol. Plant J 18: 565–570

Boursiac Y, Boudet J, Postaire O, Luu DT, Tournaire-Roux C, Maurel C (2008) Stimulus-induced downregulation of root water transport involves reactive oxygen species-activated cell signalling and plasma membrane intrinsic protein internalization. Plant J 56:207–218

Chaumont F, Barrieu F, Wojcik E, Chrispeels MJ, Jung R (2001) Aquaporins constitute a large and highly divergent protein family in maize. Plant Physiol 125:1206–1215

Daniels MJ, Mirkov TE, Chrispeels MJ (1994) The plasma membrane of *Arabidopsis thaliana* contains a mercury-insensitive aquaporin that is a homolog of the tonoplast water channel protein TIP. Plant Physiol 106:1325–1333

Dordas C, Chrispeels MJ, Brown PH (2000) Permeability and channel-mediated transport of boric acid across membrane vesicles isolated from squash roots. Plant Physiol 124:1349–1362

Fetter K, Van Wilder V, Moshelion M, Chaumont F (2004) Interactions between plasma membrane aquaporins modulate their water channel activity. Plant Cell 16:215–228

Finkelstein A (1987) Water movement through lipid bilayers, pores, and plasma membranes: theory and reality. In: Distinguished lecture series of the society of general physiologists, Vol. 4. Wiley, New York, pp 1–228

Fischer M, Kaldenhoff R (2008) On the pH regulation of plant aquaporins. J Biol Chem 283:33889–33892

Gerbeau P, Amodeo G, Henzler T, Santoni V, Ripoche P, Maurel C (2002) The water permeability of Arabidopsis plasma membrane is regulated by divalent cations and pH. Plant J 30:71–81

Gouet P, Courcelle E, Stuart DI, Metoz F (1999) ESPript: multiple sequence alignments in PostScript. Bioinformatics 15:305–308

Graber ML, DiLillo DC, Friedman BL, Pastoriza-Munoz E (1986) Characteristics of fluoroprobes for measuring intracellular pH. Anal Biochem 156(1):202–212

Hachez C, Zelazny E, Chaumont F (2006) Modulating the expression of aquaporin genes in planta: a key to understand their physiological functions? Biochim Biophys Acta 1758:1142–1156

Hachez C, Heinen RB, Draye X, Chaumont F (2008) The expression pattern of plasma membrane aquaporins in maize leaf highlights their role in hydraulic regulation. Plant Mol Biol 68:337–353

Hu CG, Hao HJ, Honda C, Kita M, Moriguchi T (2003) Putative PIP1 genes isolated from apple: expression analyses during fruit development and under osmotic stress. J Exp Bot 54:2193–2194

Javot H, Lauvergeat V, Santoni V, Martin-Laurent F, Güçlü J, Vinh J, Heyes J, Franck KI, Schäffner AR, Bouchez D, Maurel C (2003) Role of a single aquaporin isoform in root water uptake. Plant Cell 15:509–522

Johanson U, Karlsson M, Johansson I, Gustavsson S, Sjövall S, Fraysse L, Weig AR, Kjellbom P (2001) The complete set of genes encoding major intrinsic proteins in Arabidopsis provides a framework for a new nomenclature for major intrinsic proteins in plants. Plant Physiol 126:1358–1369

Johansson I, Karlsson M, Shukla VK, Chrispeels MJ, Larsson C, Kjellbom P (1998) Water transport activity of the plasma membrane aquaporin PM28A is regulated by phosphorylation. Plant Cell 10:451–459

Kammerloher W, Fischer U, Piechottka GP, Schaffner AR (1994) Water channels in the plant plasma membrane cloned by immunoselection from a mammalian expression system. Plant J 6:187–199

Karlsson M, Fotiadis D, Sjövall S, Johansson I, Hedfalk K, Engel A, Kjellbom P (2003) Reconstitution of water channel function of an aquaporin overexpressed and purified from *Pichia pastoris*. FEBS Lett 537:68–72

Kumar S, Tamura K, Nei M (2004) MEGA3: integrated software for molecular evolutionary genetics analysis and sequence alignment. Brief Bioinform 5:150–163

Larkin MA, Blackshields G, Brown NP, Chenna R, McGettigan PA, McWilliam H, Valentin F, Wallace IM, Wilm A, Lopez R, Thompson JD, Gibson TJ, Higgins DG (2007) ClustalW and ClustalX version 2. Bioinformatics 23:2947–2948

Maurel C, Tacnet F, Güclü J, Guern J, Ripoche P (1997) Purified vesicles of tobacco cell vacuolar and plasma membranes exhibit dramatically different water permeability and water channel activity. Proc Natl Acad Sci USA 94:7103–7108

Maurel C, Verdoucq L, Luu DT, Santoni V (2008) Plant aquaporins: membrane channels with multiple integrated functions. Annu Rev Plant Biol 59:595–624

Meyer MM, Verkman AS (1986) Human platelet osmotic water and nonelectrolyte transport. Am J Physiol 251:C549–C557

Moshelion M, Moran N, Chaumont F (2004) Dynamic changes in the osmotic water permeability of protoplast plasma membrane. Plant Physiol 135:2301–2317

Mut P, Bustamante C, Martínez G, Alleva K, Sutka M, Civello M, Amodeo G (2008) A fruit- specific plasma membrane aquaporin subtype PIP1;1 is regulated during strawberry (*Fragaria x ananassa*) fruit ripening. Physiol Plant 132:538–551

Niemietz CM, Tyerman SD (1997) Characterization of water channels in wheat root membrane vesicles. Plant Physiol 115:561–567

Peng ZH, Sharma V, Singleton SF, Gerson PD (2002) Synthesis and application of chain-terminating dinucleotide mRNA cap analog. Organic Lett 4:161–164

Peracchia C, Peracchia LL (2005) Inversion of both gating polarity and CO_2 sensitivity of voltage gating with D3 N mutation of Cx50. Am J Physiol Cell Physiol 288(6):C1381–C1389

Picaud S, Becq F, Dédaldéchamp F, Ageorges A, Derot S (2003) Cloning and expression of two plasma membrane aquaporins expressed during the ripening of grape berry. Funct Plant Biol 30:621–630

Postaire O, Tournaire-Roux C, Grondin A, Boursiac Y, Morillon R, Schaffner AR, Maurel C (2010) A PIP1 aquaporin contributes to hydrostatic pressure-induced water transport in both the root and rosette of Arabidopsis. Plant Physiol 152(3):1418–1430

Preston GM, Carroll TP, Guggino WB, Agre P (1992) Appearance of water channels in Xenopus oocytes expressing red cell CHIP28 protein. Science 256:385–387

Qi X, Tai CY, Wasserman BP (1995) Plasma membrane intrinsic proteins of *Beta vulgaris* L. Plant Physiol 108:387–392

Sasaki S, Ishibashi K, Nagai T, Marumo F (1992) Regulation mechanisms of intracellular pH of *Xenopus laevis* oocyte. Biochim Biophys Acta 1137(1):45–51

Stepinsky J, Waddell C, Stolarski R, Darzynkiewicz E, Rhoads RE (2001) Synthesis and properties of mRNAs containing the novel "anti-reverse" cap analog 7-methyl(3′O-methyl)GpppG and 7-methyl(3′deoxy)GpppG. RNA 7:1486–1495

Sutka M, Alleva K, Parisi M, Amodeo G (2005) Tonoplast vesicles of *Beta vulgaris* storage root show functional aquaporins regulated by protons. Biol Cell 97:837–846

Temmei Y, Uchida S, Hoshino D, Kanzawa N, Kuwahara M, Sasaki S, Tsuchiya T (2005) Water channel activities of *Mimosa pudica*

plasma membrane intrinsic proteins are regulated by direct interaction and phosphorylation. FEBS Lett 579:4417–4422

Törnroth-Horsefield S, Wang Y, Hedfalk K, Johanson U, Karlsson M, Tajkhorshid E, Neutze R, Kjellbom P (2006) Structural mechanism of plant aquaporin gating. Nature 439:688–694

Tournaire-Roux C, Sutka M, Javot H, Gout E, Gerbeau P, Luu DT, Bligny R, Maurel C (2003) Cytosolic pH regulates root water transport during anoxic stress through gating of aquaporins. Nature 425:393–397

Vandeleur RK, Mayo G, Shelden MC, Gilliham M, Kaiser BN, Tyerman SD (2009) The role of PIP aquaporins in water transport through roots: diurnal and drought stress responses reveal different strategies between isohydric and anisohydric cultivars of grapevine. Plant Physiol 149:445–460

Verdoucq L, Grondin A, Maurel C (2008) Structure-function analysis of plant aquaporin AtPIP2;1 gating by divalent cations and protons. Biochem J 415:409–416

Verkman AS, Van Hoek AN, Ma T, Frigeri A, Skach WR, Mitra A, Tamarappoo BK, Farinas J (1996) Water transport across mammalian cell membranes. Am J Physiol 270:C12–C30

Yamada S, Katsuhara M, Kelly WB, Michalowski CB, Bohnert HJ (1995) A family of transcripts encoding water channel proteins: tissue-specific expression in the common ice plant. Plant Cell 7:1129–1142

Zardoya R, Villalba S (2001) A phylogenetic framework for the aquaporin family in eukaryotes. J Mol Evol 52:391–404

Zelazny E, Borst JW, Muylaert M, Batoko H, Hemminga MA, Chaumont F (2007) FRET imaging in living maize cells reveals that plasma membrane aquaporins interact to regulate the subcellular localization. Proc Natl Acad Sci USA 104:12359–12364

Zelazny E, Miecielica U, Borst JW, Hemminga MA, Chaumont F (2009) An N-terminal diacidic motif is required for the trafficking of maize aquaporins ZmPIP2;4 and ZmPIP2;5 to the plasma membrane. Plant J 57:346–355

Zhang RB, Verkman AS (1991) Water and urea permeability properties of Xenopus oocytes: expression of mRNA from toad urinary bladder. Am J Physiol 260:C26–C34

Zhou Y, Setz N, Niemietz C, Qu H, Offler CE, Tyerman SD, Patrick JW (2007) Aquaporins and unloading of phloem-imported water in coats of developing bean seeds. Plant Cell Environ 30:1566–1577